ACCOUNTS
of chemical research

The Interface Energetics of Self-Assembled Monolayers on Metals

GEORG HEIMEL,*,†,‡ LORENZ ROMANER,†,§ EGBERT ZOJER,†,§ AND JEAN-LUC BREDAS*,†

†School of Chemistry and Biochemistry and Center for Organic Photonics and Electronics, Georgia Institute of Technology, Atlanta, Georgia 30332-0400; ‡Department of Material Science and Engineering, Massachusetts Institute of Technology, 77 Massachusetts Avenue, Cambridge, Massachusetts 02139-4307; and §Institute of Solid State Physics, Graz University of Technology, Petersgasse 16, A-8010 Graz, Austria

RECEIVED ON DECEMBER 21, 2007

CONSPECTUS

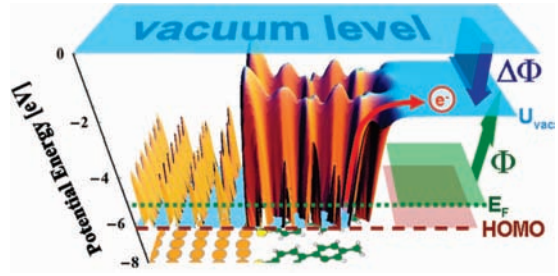

Self-assembled monolayers (SAMs) of organic molecules generally modify the surface properties when covalently linked to substrates. In organic electronics, SAMs are used to fine-tune the work functions of inorganic electrodes, thereby minimizing the energy barriers for injection or extraction of charge carriers into or out of an active organic layer; a detailed understanding of the interface energetics on an atomistic scale is required to design improved interfaces. In the field of molecular electronics, the SAM itself (or, in some cases, one or a few molecules) carries the entire device functionality; the interface then essentially becomes the device and the alignment of the molecular energy levels with those of the electrodes defines the overall charge-transport characteristics.

This Account provides a review of recent theoretical studies of the interface energetics for SAMs of π-conjugated molecules covalently linked to noble metal surfaces. After a brief description of the electrostatics of dipole layers at metal/molecule interfaces, the results of density functional theory calculations are discussed for SAMs of representative conjugated thiols on Au(111). Particular emphasis is placed on the modification of the work function of the clean metal surface upon SAM formation, the alignment of the energy levels within the SAM with the metal Fermi level, and the connection between these two quantities.

To simplify the discussion, we partition the description of the metal/SAM system into two parts by considering first an isolated free-standing layer of molecules and then the system obtained after molecule−metal bond formation. From an electrostatic standpoint, both the isolated monolayer and the metal−molecule bonds can be cast in the form of dipole layers, which lead to steps in the electrostatic potential energy at the interface. While the step due to the isolated molecular layer impacts only the work function of the SAM-covered surface, the step arising from the bond formation influences both the work function and the alignment of the electronic levels in the SAM with respect to the metal Fermi energy. Interestingly, headgroup substitutions at the far ends of the molecules forming the SAM are electrostatically decoupled from the metal−thiol interface in densely packed SAMs; as a result, the nature of these substituents and the binding chemistry between the metal and the molecules are two largely unrelated handles with which to independently tune the work function and the level alignment.

The establishment of a comprehensive atomistic picture regarding the impact of the individual components of a SAM on the interface energetics at metal/organic junctions paves the way for clear guidelines to design improved functional interfaces in organic and molecular electronics.

Published on the Web 05/29/2008 www.pubs.acs.org/acr
10.1021/ar700284q CCC: $40.75

Introduction

Single layers of organic molecules covalently bound to a surface have attracted considerable research interest over the past years.[1,2] The spontaneous assembly of molecules into densely packed and well-ordered two-dimensional crystals on a supporting substrate makes them highly suitable for modifying macroscopic surface properties[3,4] and a number of applications have been proposed for such *self-assembled monolayers* (SAMs).[5] Notably, SAMs are rapidly becoming an integral part of organic (opto)electronic devices such as, light-emitting diodes (LEDs) or field-effect transistors (FETs), where they are employed to control the energetics at the electrode/organic interface.[6–9]

The importance of the interface energetics can be easily illustrated. In Figure 1a, we show a schematic of the contact region between electrode and molecular semiconductor.[10,11] At the anode, holes are injected into the occupied states of the organic semiconductor. The energy offset between the Fermi level (E_F) and the highest occupied molecular orbital (HOMO) is commonly termed the *hole-injection barrier* (HIB),[10,11] because holes need to overcome this energy barrier before current can flow. This gives rise to an undesirable onset voltage below which the device remains inactive. At the cathode, a similar scenario is encountered for electrons.

To optimize the performance of organic electronic devices, it is critical to both reduce and balance the charge-injection barriers. Traditionally, this issue has been addressed by choosing materials with a high work function (Φ) for the anode (low E_F) and low-Φ metals (high E_F) for the cathode and by using organic semiconductors with matching energy levels. More recently, however, SAMs of dipolar organic molecules have been used to modify the effective work function of electrodes to reduce the charge-injection barriers (Figure 1b) and minimize the onset voltages.[6–8] This approach leaves more flexibility for optimizing the active device components with regard to other parameters.

SAMs are also the basis of a new class of molecular electronic devices, where individual molecules or a single monolayer are the active entity.[12–15] Here, the energy offset, ΔE, between E_F and the closest molecular orbital determines the effective height of the tunnel barrier (Figure 1c) that dominates the overall charge-transport characteristics of such single-molecule junctions.[16,17]

In view of the widely recognized role of the interfacial electronic structure in the operation of organic electronic devices, considerable experimental and theoretical efforts have been devoted to understanding the energetics at the contact, in particular between an electrode and weakly bound, physisorbed organic molecules.[10,11,18] In the present Account, we review our recent theoretical work on the interface energetics of covalently bound (i.e., strongly interacting) SAMs.[19–21] We focus on prototypical π-conjugated organic thiols, 4′-substituted 4-mercaptobiphenyls, on gold(111) surfaces and also briefly comment on the impact of varying the docking chemistry and substrate metal. On the basis of electrostatic considerations and *first-principles* calculations, we illustrate the microscopic mechanisms that give rise to the work-function modification ($\Delta\Phi$) of the Au(111) substrate and the link to the energetic alignment of the SAM frontier molecular orbitals with E_F. Our goal is to present an intuitive and comprehensive picture that can give general insight into the fundamental processes governing the interfacial phenomena in this important class of systems and that can provide valuable guidelines for the design of optimized functional interfaces.

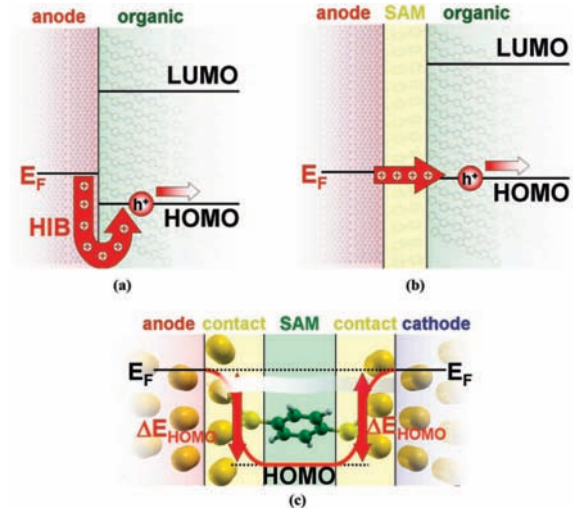

FIGURE 1. Schematic energy-level diagram at an electrode/organic interface in organic electronic devices. Part (a) shows the position of the highest occupied molecular orbital (HOMO) and the lowest unoccupied molecular orbital (LUMO) with respect to the Fermi level (E_F). By treatment of the electrode with a suitable SAM (b), the hole-injection barrier (HIB) can be reduced. In single-molecule devices (c), ΔE_{HOMO} is related to the effective height of the tunnel barrier (solid red line).

Dipole Layers and Charge Transfer

To develop a simple microscopic picture, it is useful first to consider a few model cases. In Figure 2, the solid vertical line represents an infinite two-dimensional (*xy*) plane, which plays the role of an interface and divides space into a left and a right region. We assume that the entire space is uniformly filled with a positive charge background compensated with an equally uniformly distributed negative charge.

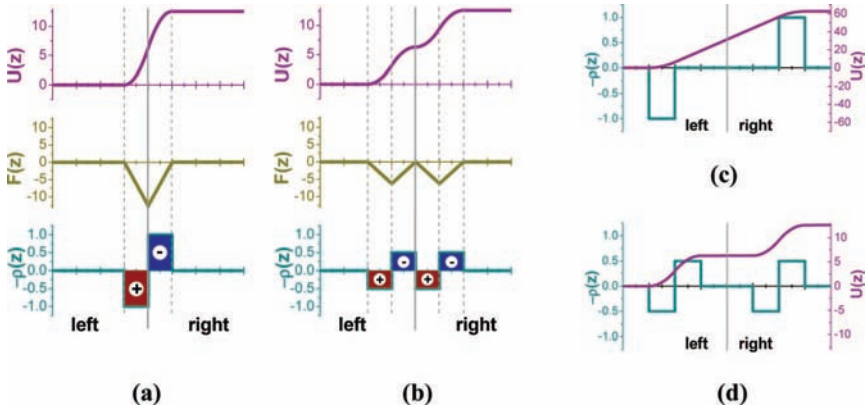

FIGURE 2. Charge density ρ (cyan), force F (brown), and potential energy U (purple) for electrons along the z-direction perpendicular to a single (a, c) and double (b, d) dipole layer. All quantities are given in atomic units. Regions of electron accumulation (−) are highlighted in blue and regions of electron depletion (+) are shown in red. The interface between the left and right half-space is marked by the solid vertical gray line.

Now, we move one electron (charge $-e$) per unit area from a layer of unit thickness on the left of the interfacial plane to a sheet of equal thickness on the right of the plane. The resulting (rectangular) charge density, $\rho(z)$, forms a 2D-infinite dipole layer, shown in the bottom panel of Figure 2a. The (triangular) electric field, $E(z)$, caused by the dipole layer can be obtained by integrating (along z) the corresponding (time-independent) Maxwell equation in one dimension:

$$\frac{dE(z)}{dz} = \frac{1}{\varepsilon_0}\rho(z) \tag{1}$$

Here, ε_0 is the vacuum permittivity; $E(z)$ multiplied with $-e$ yields the force, $F(z) = -eE(z)$, experienced by an electron at location z (center panel of Figure 2a).

Since a field can be expressed as the negative gradient of a potential, we obtain the change in electrostatic potential, $V(z)$, caused by the dipole layer via:

$$E(z) = -\frac{dV(z)}{d(z)} \tag{2}$$

$V(z)$ multiplied by $-e$ then yields the potential energy, $U(z) = -eV(z)$, of an electron at z (top panel of Figure 2a). $V(z)$ is constant away from the dipole layer but assumes different values on either side; thus, the charge transfer across the interface gives rise to a step in the electrostatic potential of magnitude ΔV or, equivalently, a step in the electron potential energy, $\Delta U = -e\Delta V$.

Combining eqs 1 and 2 leads to the Poisson equation (eq 3a), which directly relates the potential to the charge density. If one is only interested in the magnitude of ΔV, $\rho(z)$ can be expressed as the dipole moment, μ, per area, A; integration of eq 3a then yields the Helmholtz equation (eq 3b):

$$\frac{d^2V(z)}{dz^2} = -\frac{1}{\varepsilon_0}\rho(z) \tag{3a}$$

$$\Delta V = -\frac{\mu}{\varepsilon_0 A} \tag{3b}$$

It is also useful to consider two consecutive dipole layers (Figure 2b), each with half the dipole area density of the single dipole layer discussed above. While the potential energy has a slightly different shape within this double dipole layer, ΔU remains exactly the same. Importantly, this result demonstrates that *no net charge transfer across the interface is required* to establish a step in the potential energy between the left and right sides of the interface. Figure 2c,d illustrates cases where the regions of electron accumulation and depletion are at some finite distance from the interface.

The SAM as a Dipole Layer

Here, we focus on two different SAMs of 4′-X-4-mercaptobiphenyl, one with X = $-NH_2$ and one with X = $-CN$ (Figure 3b). The donor (amino) or acceptor (cyano) groups endow the molecules with sizable dipole moments pointing in opposite directions, and the thiol group binds the molecules to the gold (111) surface upon hydrogen removal. Biphenylthiols have been found to form SAMs where the molecules are arranged laterally in a typical herringbone pattern (Figure 3a);[22−24] the long axis of the molecules is slightly inclined to the surface normal by the angle θ (Figure 3b).[23,25−27]

We performed density-functional theory (DFT) calculations on these systems, employing periodic boundary conditions and the repeated-slab approach; the lateral surface unit cell is

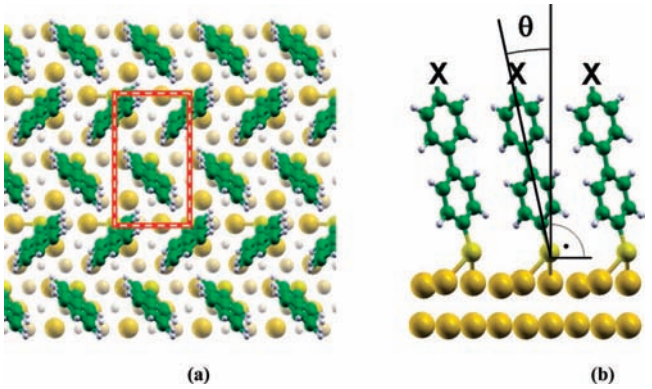

FIGURE 3. Top (a) and side (b) view of the investigated systems. The red contour in panel (a) indicates the p($\sqrt{3} \times 3$) lateral unit cell on the Au(111) surface. The angle between the long molecular axes and the surface normal is indicated by θ in panel (b); X denotes the headgroup substitutions ($-NH_2$ or $-CN$).

highlighted in Figure 3a. The methodology was detailed in ref 20, where its reliability was thoroughly assessed.

The Isolated Molecular Layer. We first consider two free-standing single layers (one with X = −CN and one with X = $-NH_2$) of molecules (in the structure they eventually assume on the surface) and turn to the interaction with the metal at a later time. Thus, at this stage, no metal is present, and the sulfur atoms are still saturated with hydrogen atoms. Molecules used to form SAMs generally possess a dipole moment; a densely packed monolayer of such molecules thus corresponds to a dipole layer in the sense of Figure 2.

In Figure 4, we show the potential energy for electrons (obtained from DFT calculations) across a single layer of the $-NH_2$ (blue) and −CN substituted (orange) biphenylthiols. In both instances, a strong difference (hereafter denoted ΔU_{vac}) is found between the values of the electrostatic potential energy in the vacuum on the thiol side (U_{vac}^{left}) and on the substituent side (U_{vac}^{right}) of the respective layer (we note that this result is consistent with the concept of *local work function* reviewed for instance in ref 10). The overall shape of the potential wells shown in Figure 4 reveals two interesting findings:

(i) If the SAM were to be seen as a dipole layer in the sense of Figure 2c (sheets of opposite charge on either side), one would expect to observe a linear slope superimposed on the potential energy well created by the ionic cores in the region of the biphenyl segment. However, this is not the case because the field created by the dipole moments of the individual molecules does not penetrate the densely packed layer.[28,29] Rather, we find that the situation is similar to that shown in Figure 2d, corresponding to (smaller) individual dipoles at each end of the SAM that are *electrostatically decoupled*; this is consistent with the observation that in their ground state, donor−acceptor substituted (push−pull) π-conjugated molecules do not exhibit any significant intramolecular charge-transfer character all the way across the π-conjugated bridge.[30]

(ii) When comparing the two monolayers, in agreement with point (i), the vacuum-level energy is seen to take the same value on the left side, dominated by the thiol groups, but differs on the right side, dominated by the amino or cyano groups.

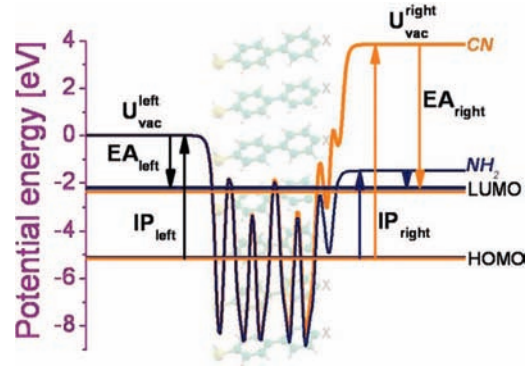

FIGURE 4. Plane-averaged potential energy for electrons across a free-standing monolayer of 4′-X-mercaptobiphenyl, one with X = $-NH_2$ (blue) and a second with X = −CN (orange). The energy differences between the HOMO or LUMO level and the vacuum level on the left side (U_{vac}^{left}) and right side (U_{vac}^{right}) of the layer correspond to the respective ionization potentials (IP_{left} and IP_{right}) and electron affinities (EA_{left} and EA_{right}).

Additionally, the field created by neighboring (dipolar) molecules *depolarizes* each molecule by inducing a dipole moment opposing the intrinsic dipole moment of the isolated individual species *in vacuo*, μ_0, or, more precisely, its projection onto the surface normal, $\mu_{0z} = \mu_0 \cos\theta$ (Figure 3b).[29,31] To estimate ΔU_{vac}, the reduced dipole moment, μ_z, and not μ_{0z} needs to be inserted into eq 3b. The depolarization can be taken into account by inserting an effective dielectric constant, ε_{eff}, into the denominator of eq 3b (i.e., $\mu_z = \mu_{0z}/\varepsilon_{eff}$);[19−21,31] ε_{eff}, however, is not to be confused with the macroscopic dielectric constant of the SAM and depends on the packing density of the molecules in the SAM, their arrangement relative to each other, and the nature of the substituents.[29,31−35]

The Ionization Potentials of SAMs. For an isolated molecule, the ionization potential (IP) is commonly understood as the energy difference between the cation, E^+, and the neutral molecule, E^0; by virtue of Koopmans theorem,[36] it is often approximated as the negative HOMO energy, E_{HOMO}:

$$IP = E^+ - E^0 \approx -E_{HOMO} \quad (4)$$

More generally, the IP is the energy difference between the final and initial states of the system. The latter is again E^0 but the former is E^+ plus the energy of the removed electron, E^{e-}:

$$IP = (E^{+} + E^{e-}) - E^{0} \approx E^{e-} - E_{HOMO} \quad (5)$$

The electrostatic potential around one isolated molecule and, thus, the potential energy of an ejected electron (E^{e-}), converges to a single value only a short distance away from the molecule. Because the origin of the energy scale can be freely chosen, this unique E^{e-} is usually set to zero and eq 4 is recovered. Thus, the IP of a single isolated molecule can be approximated by its HOMO energy only, and the removed electron need not be considered. We note that electronic relaxation, that is, screening of the hole remaining on the molecule, is not taken into account in this simplified picture.

As discussed above, the potential energy for electrons assumes different values on the left and right sides of dipolar molecular layers. In this case, it is necessary to think of IP in terms of the more general expression in eq 5. In Figure 4, the bottom horizontal lines indicate the energetic position of the HOMO in the respective SAM (orange in the case of the monolayer composed of X = −CN substituted molecules and blue in the case of X = $-NH_2$); this is the initial-state energy of the electron to be removed from the layer. Upon ionization, the electron is ejected either over the thiol (left) side or the substituent (right) side. Because the final-state energies of the electron (E^{e-}) for these two cases are different (either U_{vac}^{left} or U_{vac}^{right}), each molecular layer has two ionization potentials, IP_{right} and IP_{left}, with their difference equal to ΔU_{vac}. For the electron affinities (EA), similar considerations hold but involve the lowest unoccupied molecular orbital (LUMO). Again, the screening of the hole remaining in the layer, via local polarization of the surrounding molecules, is not taken into account here.

In Figure 4, IP_{left} is seen to be nearly identical whatever the nature of the substituents while IP_{right} is markedly different; thus, the 4′-substitution only affects the right end of the layers, which is another manifestation of the efficient electrostatic screening within the SAM.[28,29] We have also compared molecular layers with different docking groups, thiol (−SH), pyridine, and isocyanide (−NC), but with the same simple hydrogen termination at the 4′-position (thus having chemically identical "right sides").[21] In these instances, the SAMs are found to be electronically equivalent on the right side whereas IP_{left} assumes markedly different values.[21] These results should be borne in mind when turning to the metal/SAM interface in the next section.

The Metal/SAM Interface

Surface Dipole, Push-Back, and Interface Dipole. Before we focus in more detail on the process of bond formation between the molecular layer and a metal surface, we need to recall a common phenomenon encountered when adsorbing molecules onto metal surfaces.[10,11,37–39] Consider the simplified picture of a metal surface shown in Figure 5a: The ionic cores in the metal are assumed to give rise to a square potential well for the electrons and all states are filled up to the Fermi level, E_F.[37] The energy difference between E_F and the potential energy of an electron in the vacuum above this hypothetical surface, U_{vac}, could be referred to as the *intrinsic* work function, $\tilde{\Phi}$, (or chemical potential) of the metal. However, because the potential well is not infinitely deep, there is a finite probability of finding electrons outside the potential well, that is, electron density is "leaking out" from the metal into the vacuum (Figure 5b).[37] Consequently, a dipole layer in the sense of Figure 2a is formed with a negatively charged region just above the metal surface and a positively charged region beneath. This dipole layer is commonly referred to as the *surface dipole* and gives rise to a potential step across the metal surface. The surface dipole raises U_{vac} directly above the metal surface relative to E_F and leads to the *observed* work function, Φ, of the metal surface.[37]

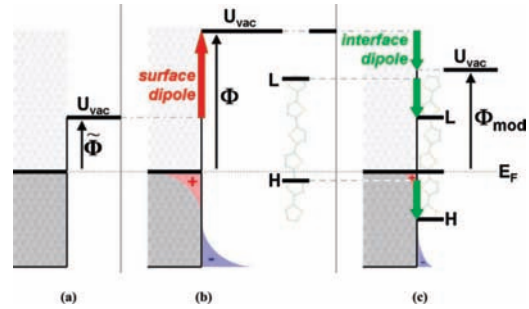

FIGURE 5. (a) Model of a metal surface (square potential well in the absence of a surface dipole; all electronic states are occupied up to the Fermi level (E_F). Also shown is the vacuum level (U_{vac}) above the surface; the difference between E_F and U_{vac} is the (hypothetical) intrinsic work function, $\tilde{\Phi}$. (b) As electrons leak out of the potential well (blue region) and leave a positively charged region below the surface (red), a *surface dipole* is formed, which raises U_{vac} and leads to the observed work function, Φ. Also shown are the HOMO (H) and LUMO (L) levels of a molecule at some distance from the surface. (c) Upon interaction of the molecules, the electrons are pushed back into the metal, reducing the surface dipole; U_{vac} and all molecular orbitals are lowered in energy with respect to E_F, leading to the modified work function (Φ_{mod}) and modified charge-carrier injection barriers.

We now turn to the situation where a molecule appears at some distance from this surface (Figure 5b). By matching its IP with Φ, one could hope for a vanishing hole-injection barrier (Figure 1a,b). However, upon deposition of even only weakly interacting (physisorbed) species (e.g., organic π-conjugated molecules[10,11] or noble gas atoms[38,39]), the electron cloud leaking out of the metal surface is pushed back into the met-

al.[40] This *push-back* (or *pillow*) effect always contributes to reduce the surface dipole and lower U_{vac} relative to E_F and, consequently, leads to a reduced work function, Φ_{mod}, of the sample (Figure 5c). In the case of physisorbed molecules, the amount by which the surface dipole is reduced is often termed the *interface dipole*. As such an interface dipole occurs between the metal and the adsorbate; not only U_{vac} but also all electronic states in the adsorbate (in particular, the HOMO) are lowered in energy with respect to E_F (Figure 5c).[10,11] This always increases the hole-injection barrier (Figure 1a) and is thus detrimental for the performance of organic electronic devices relying on the active organic layer being directly deposited onto a metal electrode. As discussed in the next section, however, SAMs of suitable molecules can counteract this effect and lower the HIB by effectively *increasing* the metal work function ($\Phi_{mod} > \Phi$) and by presenting a (modified) surface to subsequently deposited organics at which no such push-back occurs.[41]

Bond Formation between SAM and Metal. When a thiol SAM is deposited on the metal surface, interacts, and establishes chemical bonds, the modification of the charge density at the metal−SAM interface originates in two contributions: (i) since sulfur atoms appear in the immediate vicinity of the Au(111) surface (ca. 2.3 Å), the push-back effect[38−40] described above occurs; (ii) in addition, the S−H bonds are replaced by bonds between sulfur and gold. These two contributions add up, and the total rearrangement of the charge density, $\Delta\rho$, can be obtained from DFT calculations as:[19−21]

$$\Delta\rho = \rho - [(\rho_{mol} - \rho_H) + \rho_{Au}] \quad (6)$$

Here, ρ is the charge density of the final system [SAM on Au(111)]; ρ_{mol} is the charge density of the isolated, H-saturated thiol molecular layer discussed earlier; ρ_H is the charge density associated with the hydrogen atoms that are removed upon adsorption; and ρ_{Au} is the charge density of the clean Au(111) surface. The bottom panel of Figure 6 shows $\Delta\rho$ integrated in the *xy*-plane, $\Delta\rho(z)$, for the SAMs of two 4′-substituted 4-mercaptobiphenyls on gold.

The most striking features from Figure 6 are that (i) $\Delta\rho(z)$ is confined to the immediate interface region, (ii) $\Delta\rho(z)$ is identical for the two types of SAMs (these first two points are a consequence of the dielectric screening within the molecular layer and hold only in densely packed SAMs[28,29,31]), and (iii) no significant net charge transfer occurs between the metal and the molecular layer. Interestingly, the bottom panel in Figure 6 is reminiscent of the situation depicted in Figure 2b, with no net charge transfer across the metal−molecule interface

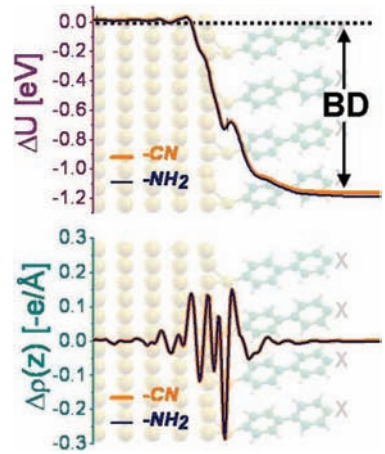

FIGURE 6. Charge-density difference ($\Delta\rho$, bottom) upon metal/SAM bond formation for 4′-X-4-mercaptobiphenyl with X = $-NH_2$ and −CN and resulting change in the potential energy of an electron (ΔU, top) at the interface, referred to as the bond dipole (BD).

and regions of electron accumulation and depletion alternating at the (sub)bond-length scale. Integrating eq 3a yields the potential (energy) step due to $\Delta\rho(z)$ (top panel in Figure 6) (which, in our calculations, corresponds to a potential drop by 1.2 eV). Thus, upon metal−SAM bond formation, the entire potential well of the SAM and U_{vac}^{right} (Figure 4) are rigidly shifted in energy with respect to E_F. In analogy to the interface dipole, a terminology mainly used in conjunction with physisorbed molecules, we refer here to the step in potential energy at the SAM/metal interface as the *bond dipole* (BD). We stress that BD can change dramatically in both magnitude and sign when, instead of thiols, a different docking chemistry is used (e.g., in the case of pyridine, a drop by 0.6 eV is calculated and in the case of isocyanide an increase by 1.3 eV).[21] Furthermore, BD depends on the packing density of the molecules in the SAM and, at low coverage, also on the 4′-substituents.[31]

Work-Function Modification and Level Alignment

The stage is now set to establish an atomistic picture of the mechanisms that determine the work-function modification of the clean Au(111) surface upon SAM formation and the alignment of the frontier molecular orbitals in the SAM with E_F. The overall process is schematically shown in Figure 7 in the case of the −CN substituted biphenylthiol.

Work-Function Modification. For the clean gold surface, $\Phi_{Au(111)}$ denotes the energy required to promote one electron from E_F to the vacuum level above the surface (Figure 7a). The SAM deposition has two consequences: (i) the ejected electron needs to overcome the additional potential step created by the dipolar molecular layer, ΔU_{vac}, to reach the vac-

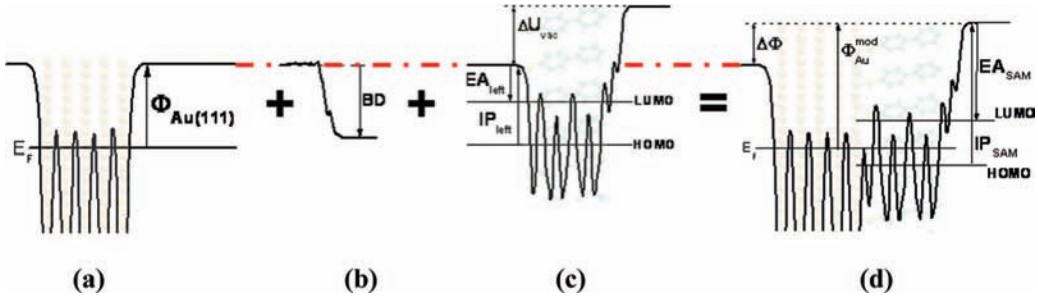

FIGURE 7. The work function, $\Phi_{Au(111)}$, of the clean gold surface (a) is the difference between the Fermi energy (E_F) and the vacuum level (horizontal dash-dotted red line). Upon monolayer formation, the potential well of the SAM (c) is shifted by the bond dipole, BD (b), relative to E_F leading to the final situation in panel d. Also indicated are the potential energy step, ΔU_{vac}, across the dipolar SAM (c), the HOMO, the LUMO, and the left-side ionization potential (IP_{left}) and electron affinity (EA_{left}). In panel (d), the modified work function, Φ_{Au}^{mod}, and the difference from $\Phi_{Au(111)}$, $\Delta\Phi$, is indicated together with the ionization potential (IP_{SAM}) and electron affinity (EA_{SAM}) of the SAM.

TABLE 1. Potential Energy Step across the Isolated Molecular Monolayer, ΔU_{vac}, and across the Metal–SAM Interface, BD, and the Resulting Modification, $\Delta\Phi$, of the Work Function[a] of the Clean Substrate

system[b]	ΔV_{vac} [eV]	BD [eV]	$\Delta\Phi$ [eV]
Au|S|2P|NH_2	−1.49	−1.20	−2.69
Au|S|2P|CN	3.84	−1.18	2.65
Au|S|2P|H	−0.37	−1.17	−1.55
Ag|S|2P|H	−0.38	−0.39	−0.77
Au|CN|2P|H	−3.40	1.28	−2.12

[a] Calculated to be 5.2 eV for clean Au(111) and 4.5 eV for clean Ag(111). [b] The systems are 4′-amino-4-mercaptobiphenyl (Au|S|2P|NH_2), 4′-cyano-4-mercaptobiphenyl (Au|S|2P|CN), 4-mercaptobiphenyl (Au|S|2P|H), and 4-isocyanide-biphenyl (Au|CN|2P|H) on gold, as well as 4-mercaptobiphenyl (Ag|S|2P|H) on silver.

uum level above the SAM (Figure 7c); (ii) the bond formation between SAM and metal shifts the potential well of the SAM relative to E_F by BD (Figure 7b). The total work-function modification, $\Delta\Phi$, can thus be written as:[19–21]

$$\Delta\Phi = \Delta U_{vac} + BD \quad (7)$$

As shown in Figure 7d, the modified work function, $\Phi_{Au}^{mod} = \Phi_{Au(111)} + \Delta\Phi$, is significantly higher than $\Phi_{Au(111)}$ (Figure 7a) in the case of the −CN substitution, which would contribute to a reduced hole-injection barrier in organic electronic devices (Figure 1b). The $-NH_2$ substitution leads to a highly reduced work function, a scenario that would lower the barrier for injection of electrons from a SAM-treated cathode into the active organic layer of the device. In Table 1, we list the calculated ΔV_{vac}, BD, and $\Delta\Phi$ values for the two systems explicitly discussed in the present Account [(4′-amino- and 4′-cyano-4-mercaptobiphenyl on Au(111)]. Also shown are the values for unsubstituted 4-mercaptobiphenyl on gold with both a thiol and an isocyanide docking group (to highlight the impact of the docking chemistry on BD) as well as unsubstituted 4-mercaptobiphenyl on silver.[21] Interestingly, the BD calculated for 4-mercaptobiphenyl on Ag (−0.4 eV) is 0.8 eV lower than that on Au (−1.2 eV) and thus nearly completely compensates the work-function difference (0.7 eV) between the clean (111) surfaces of the two metals (calculated to be 4.5 eV for Ag and 5.2 eV for Au). Thus, when the same thiols are deposited on Ag(111) and Au(111), the work functions of the covered surfaces are expected to be the same. This has actually been confirmed by data from Kelvin-probe measurements carried out by de Boer and co-workers.[8]

Level Alignment. Prior to establishing the covalent bonds between metal and SAM, the energy difference between HOMO and E_F is given by the difference between the work function of the clean gold surface, $\Phi_{Au(111)}$, and IP_{left} (Figure 7a,c). Upon bond formation, BD shifts the potential well of the SAM and all corresponding energy levels relative to E_F (Figure 7b). The final energy separation, ΔE_{HOMO}, in the combined metal/SAM system (Figure 7d) is then given by:

$$\Delta E_{HOMO} = \Phi_{Au(111)} - IP_{left} + BD \quad (8)$$

Note that because $\rho(z)$ has a small but finite tail on the first phenylene ring of the molecule (Figure 6), the electronic structure of the bound SAM is slightly perturbed compared to the free-standing molecular layer. This generally leads to a small corrective term for ΔE_{HOMO} which needs to be added to the right-hand side of eq 8.[19–21] The alignment of the LUMO with E_F is obtained by substituting IP_{left} with EA_{left}.[19–21]

Importantly, since the dipole fields generated by the head groups do not penetrate the densely packed SAM, we find the same ΔE_{HOMO} for the cyano- and amino-substituted SAMs despite the strongly different IPs of the isolated molecules.[19] Thus, chemical substitutions outside the immediate metal/SAM interface (i.e., the docking group and the first phenylene ring) cannot be expected to impact significantly the tunnel barrier in single-molecule devices (unless they affect the packing density of molecules on the surface[31]).

Conclusion

We have presented a comprehensive, microscopic picture for the interface energetics of self-assembled monolayers on metals and focused on aspects relevant for the application of these systems in organic electronic devices. In view of basic electrostatic considerations on single and multiple dipole layers, we discussed the results of DFT calculations for the prototypical case of 4′-X-4-mercaptobiphenyls on gold with X = $-NH_2$ and −CN. For free-standing molecular monolayers, the concept of right- and left-side ionization potentials in dipolar SAMs was established. Electrostatic interactions between the two sides of a densely packed SAM were seen to be largely suppressed. After reviewing more general interfacial phenomena at metal/molecule junctions, we provided a detailed analysis of the bonding-induced charge rearrangements that occur upon SAM formation. Importantly, no indication is found for any significant net charge transfer between metal and molecules, and due to dielectric screening, the S−Au bond appears to be insensitive to the headgroup substitutions, X, at high coverage.

The modification of the work function of the clean Au(111) surface (relevant for optimizing charge-injection barriers in organic electronic devices) and the energetic alignment of the frontier molecular orbitals in the SAM with the electrode Fermi level (relevant for single-molecule devices) were decomposed into contributions from two dipole layers; one, the bond dipole, is formed at the immediate gold−sulfur interface, while the second is due to the aligned dipole moments of the molecules within the SAM. The step in electrostatic potential energy due to the former is seen to impact both level alignment and work-function modification, while the potential step arising from the latter contributes to the work-function modification only. Importantly, the choices of the docking chemistry and headgroup substitution allow for an *independent* optimization of those interfacial properties of the electrode/organic contact that critically contribute to the performance and functionality of organic devices.

G.H. acknowledges financial support from the INSANE Marie-Curie Project 021511 of the European Commission. The work at Georgia Tech has been partly supported by the Office of Naval Research, the Department of Energy, and the National Science Foundation (under the CRIF Program Award CHE-0443564 and the STC Program Award DMR-0120967).

BIOGRAPHICAL INFORMATION

Georg Heimel received his Ph.D. (2003) from the Institute of Solid State Physics at the Graz University of Technology, Austria. His postdoctoral work at the Georgia Institute of Technology and currently at MIT deals with the modeling of interfaces in organic and molecular electronics.

Lorenz Romaner obtained his Ph.D. (2007) from the Institute of Solid State Physics at the Graz University of Technology. During his Ph.D., he spent two years at Georgia Tech. He currently holds a postdoctoral position at the University of Leoben, Austria, where his theoretical research revolves around the study of molecules adsorbed on metallic surfaces and the mechanical properties of metals and alloys.

Egbert Zojer received his Ph.D. in Physics (1999) from the Graz University of Technology, where he was appointed Associate Professor in 2002. On a leave from Graz, he worked for one year (2002−2003) as an Assistant Staff Scientist at the University of Arizona and for two years (2003−2005) as a Senior Research Scientist at Georgia Tech. His current research focuses on the experimental and computational investigation of organic/inorganic interfaces as well as on the description of excitation processes in conjugated organic systems.

Jean-Luc Bredas received his Ph.D. in Chemistry in 1979 from the University of Namur, Belgium. After a postdoctoral stay at MIT (1980−1981), he went back to Namur as a Research Fellow of the Belgian National Science Foundation. In 1988, he was appointed Professor at the University of Mons-Hainaut, Belgium, where he established the Laboratory for Chemistry of Novel Materials. He joined the University of Arizona in 1999 before moving to Georgia Tech in 2003 where he is Professor of Chemistry and Biochemistry and the Georgia Research Alliance Eminent Scholar and Chair in Molecular Design. His research focuses on the computational design of novel organic materials.

FOOTNOTES

*To whom correspondence should be addressed. GH: e-mail, georg.heimel@physik.hu-berlin.de. JLB: e-mail, jean-luc.bredas@chemistry.gatech.edu.

REFERENCES

1 Ulman, A. Formation and Structure of Self-Assembled Monolayers. *Chem. Rev.* **1996**, *96*, 1533–1554.

2 Love, J. C.; Estroff, L. A.; Kriebel, J. K.; Nuzzo, R. G.; Whitesides, G. M. Self-Assembled Monolayers of Thiolates on Metals as a Form of Nanotechnology. *Chem. Rev.* **2005**, *105*, 1103–1169.

3 Jennings, G. K.; Laibinis, P. E. Self-Assembled Monolayers of Alkanethiols on Copper Provide Corrosion Resistance in Aqueous Environments. *Colloids Surf., A* **1996**, *116*, 105–114.

4 Genzer, J.; Efimenko, K. Creating Long-Lived Superhydrophobic Polymer Surfaces Through Mechanically Assembled Monolayers. *Science* **2000**, *290*, 2130–2133.

5 Gooding, J. J.; Mearns, F.; Yang, W. R.; Liu, J. Q. Self-Assembled Monolayers into the 21(st) Century: Recent Advances and Applications. *Electroanalysis* **2003**, *15*, 81–96.

6 Campbell, I. H.; Rubin, S.; Zawodzinski, T. A.; Kress, J. D.; Martin, R. L.; Smith, D. L.; Barashkov, N. N.; Ferraris, J. P. Controlling Schottky Energy Barriers in Organic Electronic Devices Using Self-Assembled Monolayers. *Phys. Rev. B* **1996**, *54*, 14321–14324.

7 Ganzorig, C.; Kwak, K. J.; Yagi, K.; Fujihira, M. Fine Tuning Work Function of Indium Tin Oxide by Surface Molecular Design: Enhanced Hole Injection in Organic Electroluminescent Devices. *Appl. Phys. Lett.* **2001**, *79*, 272–274.

8 de Boer, B.; Hadipour, A.; Mandoc, M. M.; van Woudenbergh, T.; Blom, P. W. M. Tuning of Metal Work Functions with Self-Assembled Monolayers. *Adv. Mater.* **2005**, *17*, 621–625.

9 Bock, C.; Pham, D. V.; Kunze, U.; Kafer, D.; Witte, G.; Woll, C. Improved Morphology and Charge Carrier Injection in Pentacene Field-Effect Transistors with Thiol-Treated Electrodes. *J. Appl. Phys.* **2006**, *100*, 114517.

10 Ishii, H.; Sugiyama, K.; Ito, E.; Seki, K. Energy Level Alignment and Interfacial Electronic Structures at Organic/Metal and Organic/Organic Interfaces. *Adv. Mater.* **1999**, *11*, 605–625.

11 Kahn, A.; Koch, N.; Gao, W. Y. Electronic Structure and Electrical Properties of Interfaces between Metals and π-Conjugated Molecular Films. *J. Polym. Sci., Part B* **2003**, *41*, 2529–2548.

12 Bumm, L. A.; Arnold, J. J.; Cygan, M. T.; Dunbar, T. D.; Burgin, T. P.; Jones, L.; Allara, D. L.; Tour, J. M.; Weiss, P. S. Are Single Molecular Wires Conducting? *Science* **1996**, *271*, 1705–1707.

13 Chen, J.; Reed, M. A.; Rawlett, A. M.; Tour, J. M. Large On-Off Ratios and Negative Differential Resistance in a Molecular Electronic Device. *Science* **1999**, *286*, 1550–1552.

14 Park, J.; Pasupathy, A. N.; Goldsmith, J. I.; Chang, C.; Yaish, Y.; Petta, J. R.; Rinkoski, M.; Sethna, J. P.; Abruna, H. D.; McEuen, P. L.; Ralph, D. C. Coulomb Blockade and the Kondo Effect in Single-Atom Transistors. *Nature* **2002**, *417*, 722–725.

15 Akkerman, H. B.; Blom, P. W. M.; de Leeuw, D. M.; de Boer, B. Towards Molecular Electronics with Large-Area Molecular Junctions. *Nature* **2006**, *441*, 69–72.

16 Vondrak, T.; Wang, H.; Winget, P.; Cramer, C. J.; Zhu, X. Y. Interfacial Electronic Structure in Thiolate Self-Assembled Monolayers: Implication for Molecular Electronics. *J. Am. Chem. Soc.* **2000**, *122*, 4700–4707.

17 Xue, Y. Q.; Datta, S.; Ratner, M. A. Charge Transfer and "Band Lineup" in Molecular Electronic Devices: A Chemical and Numerical Interpretation. *J. Chem. Phys.* **2001**, *115*, 4292–4299.

18 Vásquez, H.; Flores, F.; Oszwaldowski, R.; Ortega, J.; Pérez, R.; Kahn, A. Barrier Formation at Metal-Organic Interfaces: Dipole Formation and the Charge Neutrality Level. *Appl. Surf. Sci.* **2004**, *234*, 107–112.

19 Heimel, G.; Romaner, L.; Bredas, J. L.; Zojer, E. Interface Energetics and Level Alignment at Covalent Metal-Molecule Junctions: π-Conjugated Thiols on Gold. *Phys. Rev. Lett.* **2006**, *96*, 196806.

20 Heimel, G.; Romaner, L.; Bredas, J. L.; Zojer, E. Organic/Metal Interfaces in Self-Assembled Monolayers of Conjugated Thiols: A First-Principles Benchmark Study. *Surf. Sci.* **2006**, *600*, 4548–4562.

21 Heimel, G.; Romaner, L.; Zojer, E.; Bredas, J. L. Toward Control of the Metal-Organic Interfacial Electronic Structure in Molecular Electronics: A First-Principles Study on Self-Assembled Monolayers of π-Conjugated Molecules on Noble Metals. *Nano Lett.* **2007**, *7*, 932–940.

22 Tao, Y. T.; Wu, C. C.; Eu, J. Y.; Lin, W. L.; Wu, K. C.; Chen, C. H. Structure Evolution of Aromatic-Derivatized Thiol Monolayers on Evaporated Gold. *Langmuir* **1997**, *13*, 4018–4023.

23 Leung, T. Y. B.; Schwartz, P.; Scoles, G.; Schreiber, F.; Ulman, A. Structure and Growth of 4-Methyl-4′-mercaptobiphenyl Monolayers on Au(111): A Surface Diffraction Study. *Surf. Sci.* **2000**, *458*, 34–52.

24 Azzam, W.; Fuxen, C.; Birkner, A.; Rong, H. T.; Buck, M.; Wöll, C. Coexistence of Different Structural Phases in Thioaromatic Monolayers on Au(111). *Langmuir* **2003**, *19*, 4958–4968.

25 Frey, S.; Stadler, V.; Heister, K.; Eck, W.; Zharnikov, M.; Grunze, M.; Zeysing, B.; Terfort, A. Structure of Thioaromatic Self-Assembled Monolayers on Gold and Silver. *Langmuir* **2001**, *17*, 2408–2415.

26 Kang, J. F.; Ulman, A.; Liao, S.; Jordan, R.; Yang, G. H.; Liu, G. Y. Self-Assembled Rigid Monolayers of 4′-Substituted-4-Mercaptobiphenyls on Gold and Silver Surfaces. *Langmuir* **2001**, *17*, 95–106.

27 Shaporenko, A.; Heister, K.; Ulman, A.; Grunze, M.; Zharnikov, M. The Effect of Halogen Substitution in Self-Assembled Monolayers of 4-Mercaptobiphenyls on Noble Metal Substrates. *J. Phys. Chem. B* **2005**, *109*, 4096–4103.

28 Natan, A.; Kronik, L.; Haick, H.; Tung, R. T. Electrostatic Properties of Ideal and Non-ideal Polar Organic Monolayers: Implications for Electronic Devices. *Adv. Mater.* **2007**, *19*, 4103–4117.

29 Deutsch, D.; Natan, A.; Shapira, Y.; Kronik, L. Electrostatic Properties of Adsorbed Polar Molecules: Opposite Behavior of a Single Molecule and a Molecular Monolayer. *J. Am. Chem. Soc.* **2007**, *129*, 2989–2997.

30 Meyers, F.; Bredas, J. L. On the Nature of the Ground State in Push-Pull Conjugated Molecules with Large Quadratic Optical Nonlinearities: From Paranitroaniline to P-Nitro-p′-aminodiphenyl-hexatriyne. *Nonlinear Opt.* **1991**, *1*, 119–123.

31 Romaner, L.; Heimel, G.; Zojer, E. Electronic Structure of Thiol-Bonded Self-Assembled Monolayers: Impact of Coverage. *Phys. Rev. B* **2008**, *77*, 045113.

32 Topping, J. On the Mutual Potential Energy of a Plane Network of Doublets. *Proc. R. Soc. London, Ser. A* **1927**, *114*, 67–72.

33 Maschhoff, B. L.; Cowin, J. P. Corrected Electrostatic Model for Dipoles Adsorbed on a Metal-Surface. *J. Chem. Phys.* **1994**, *101*, 8138–8151.

34 Iwamoto, M.; Mizutani, Y.; Sugimura, A. Calculation of the Dielectric Constant of Monolayer Films on a Material Surface. *Phys. Rev. B* **1996**, *54*, 8186–8190.

35 Cornil, D.; Olivier, Y.; Geskin, V.; Cornil, J. Depolarization Effects in Self-Assembled Monolayers: A Quantum-Chemical Insight. *Adv. Funct. Mater.* **2007**, *17*, 1143–1148.

36 Janak, J. F. Proof That $dE/dn_i = \epsilon_i$ in Density-Functional Theory. *Phys. Rev. B* **1978**, *18*, 7165–7168.

37 Lang, N. D.; Kohn, W. Theory of Metal Surfaces: Work Function. *Phys. Rev. B* **1971**, *3*, 1215–1223.

38 Lang, N. D. Interaction between Closed-Shell Systems and Metal-Surfaces. *Phys. Rev. Lett.* **1981**, *46*, 842–845.

39 Chen, Y. C.; Cunningham, J. E.; Flynn, C. P. Dependence of Rare-Gas-Adsorbate Dipole-Moment on Substrate Work Function. *Phys. Rev. B* **1984**, *30*, 7317–7319.

40 Witte, G.; Lukas, S.; Bagus, P. S.; Wöll, C. Vacuum Level Alignment at Organic/Metal Junctions: "Cushion" Effect and the Interface Dipole. *Appl. Phys. Lett.* **2005**, *87*, 263502.

41 Koch, N.; Elschner, A.; Schwartz, J.; Kahn, A. Organic Molecular Films on Gold versus Conducting Polymer: Influence of Injection Barrier Height and Morphology on Current-Voltage Characteristics. *Appl. Phys. Lett.* **2003**, *82*, 2281–2283 .